Automatica 152 (2023) 110997

Contents lists available at ScienceDirect

Automatica

journal homepage: www.elsevier.com/locate/automatica

Brief paper

Prescribed-time formation tracking of second-order multi-agent networks with directed graphs☆

Teng-Fei Ding [a], Ming-Feng Ge [a,*], Caihua Xiong [b], Zhi-Wei Liu [c], Guang Ling [d]

[a] School of Mechanical Engineering and Electronic Information, China University of Geosciences, Wuhan, 430074, PR China
[b] State Key Laboratory of Digital Manufacturing Equipment and Technology, School of Mechanical Science and Engineering, Huazhong University of Science and Technology, Wuhan, 430074, PR China
[c] School of Artificial Intelligence and Automation, Huazhong University of Science and Technology, Wuhan, 430074, PR China
[d] School of Science, Wuhan University of Technology, Wuhan 430070, PR China

ARTICLE INFO

Article history:
Received 6 May 2021
Received in revised form 29 October 2022
Accepted 26 February 2023
Available online 31 March 2023

Keywords:
Prescribed-time observer-based control
Formation tracking
Multi-agent network (MAN)
Directed graphs

ABSTRACT

The objective of this paper is to solve the prescribed-time formation tracking problem for the second-order multi-agent network (MAN) with the interaction graph containing a directed spanning tree. By introducing a time-varying function, a novel prescribed-time observer-based control algorithm is presented for driving all the followers to approach a dynamic leader within the prescribed time, which can be pre-specified as a user-designed parameter in the algorithm and is regardless of the initial condition. Especially, the prescribed-time state observer, as an important component of the algorithm, is newly designed to estimate the states of the leader in a distributed manner and also within a user-determined prescribed time. In order to establish the prescribed-time convergence of the closed-loop system in the cascade form, we design a new Lyapunov function candidate and then derive the corresponding sufficient conditions for prescribed-time stability of the error states. Finally, several numerical examples are performed on six agents to verify the effectiveness of the presented algorithm.

1. Introduction

In recent years, distributed control of multi-agent networks (MANs) has become an important research topic in the field of robotics and automation (Ge, Liu, Wen, Yu, & Huang, 2020; Ren & Beard, 2005). The control algorithms for formation tracking have been recognized as one of the most significant concerns, due to their wide applications in regulating networked mobile robots (Liang et al., 2016; Yoo & Kim, 2015), networked marine surface vehicles (Liang, Ge, Liu, Ling, & Liu, 2020), and other multi-robot systems (Ding, Ge, Liu, Wang, & Karimi, 2020).

Besides, the convergence time of MANs is a key index for evaluating the performance of the distributed control algorithms. In the early stages, the convergence time of the distributed control and observer algorithms is *infinity*, namely, the error states converge to the origin as time goes to infinity (Olfati-Saber & Murray, 2004). It thus motivates people to develop *finite-time* distributed control and observer algorithms for achieving different collective behaviors, including consensus (Khoo, Xie, & Man, 2009; L, Du, & Lin, 2011; Zhao & Hua, 2014) and formation tracking (Ge, Guan, Yang, Li, & Wang, 2016; Hua, Dong, Liang, Li, & Ren, 2020; Xiao, Wang, Chen, & Gao, 2009). In Wang, Yuan, and Liu (2021), by employing the state observer to recover the disturbances, the leader-following output consensus problem has been addressed in a finite time. Some novel finite- and fixed-time average tracking algorithms have been proposed in Wen, Yu, Fu, Wang, and Yu (2021), where the fast distributed average tracking problem of MANs has been successfully solved. Note that the convergence time of all the above-mentioned results is determined by the initial condition and the control parameters. In practical applications, it is not easy to obtain the accurate initial condition of the MANs; meanwhile, the convergence time may be too great if the initial value is too big. To overcome these shortcomings, some outstanding works about the *fixed-time* control and observer approaches have been presented in Polyakov (2012) and Zuo (2014, 2015), in which the convergence time is independent of the initial condition. Thus, fruitful results have been obtained based on the fixed-time control approaches (Hong, Yu, Wen, & Yu, 2017; Lv, Wen, & Huang, 2020; Yang & Ye, 2020; You, Hua, Li, & Jia, 2020). In Tian, Lu, Zuo, and Yang

☆ The material in this paper was not presented at any conference. This paper was recommended for publication in revised form by Associate Editor Chanying Li under the direction of Editor Miroslav Krstic.

* Corresponding author.
E-mail addresses: dingtf@cug.edu.cn (T.-F. Ding), gemf@cug.edu.cn (M.-F. Ge), chxiong@hust.edu.cn (C. Xiong), zwliu@hust.edu.cn (Z.-W. Liu), guangling@whut.edu.cn (G. Ling).

https://doi.org/10.1016/j.automatica.2023.110997
0005-1098/

(2019), the novel observer-based algorithm has been developed to solve the leader-follow consensus in a fixed time without velocity measurement. In Du, Wen, Wu, Cheng, and Lu (2020), the distributed fixed-time consensus problem of heterogeneous nonlinear MANs has been addressed by designing the distributed fixed-time observers and tracking controllers. By means of event-triggered mechanism, the formation tracking problem has been addressed in a fixed time (Cai, Zhang, Wang, Zhang, & He, 2021). However, the convergence time of the fixed-time control and observer approaches cannot be specified arbitrarily since it has a complex relationship with multiple control parameters.

Thus, people begun to develop a simpler way to *prescribe* the convergence time by selecting the controller and observer parameters, being referred to as *prescribed-time* control. In the pioneer work of this area, an important time-varying function has been proposed to construct the prescribed-time control for stabilizing a class of nonlinear systems (Song, Wang, Holloway, & Krstic, 2017). More recently, the key ways of prescribed-time control and observer have been developed for generalized linear systems (Holloway & Krstic, 2019a, 2019b). This then motivates the development of distributed algorithms for controlling and observing the MANs in a prescribed time (Chen, Yu, & Hao, 2020; Ren, Zhou, Li, Liu, & Sun, 2021; Wang, Song, Hill, & Krstic, 2019). There also exist some other distributed algorithms focusing on prescription of the convergence time (Ning, Han, & Zuo, 2019). However, such prescribed-time control algorithms are mainly based on the assumption that the interaction graph is undirected and connected (Chen et al., 2020; Ni, Liu, Tang, & Liu, 2021; Ning et al., 2019; Wang et al., 2019) or the sliding mode approaches inevitably leading to chattering (Liang et al., 2020; Ni et al., 2021; Ning, Han, & Zuo, 2021). It still lacks an effective and less conservative approach for prescribing the convergence time of the second-order MAN, whose interaction graph is directed and contains a spanning tree.

This paper investigates the prescribed-time formation tracking of the second-order MAN with a directed spanning tree. The main contributions are summarized as follows.

(1) Different from the prescribed-time control algorithms for the first-order MAN with the undirected and connected graph (Wang et al., 2019), we newly designed the prescribed-time observer-based control algorithms for the second-order MAN with a less conservative graph assumption, namely, the directed graph contains a spanning tree. Besides, the convergence time of the presented algorithm is independent of the initial condition, unlike that of the control algorithms depending on the initial condition provided in Ning et al. (2021).
(2) Different from the result proposed in Ren et al. (2021), the newly constructed Lyapunov function is less conservative such that the sufficient condition for stability of the closed-loop system is simpler and to some degree milder. Besides, it makes the selection of the corresponding control parameters much easier.
(3) We present a simpler way to choose only one parameter that admits the user to prescribe the convergence time of the MANs in a more general case (i.e., less conservative graph condition), where the related results are much more complex (Ni et al., 2021; Ning & Han, 2019).

The rest parts of this paper are outlined as follows. Section 2 gives some preliminaries. Section 3 provides the designed algorithm and the stability analysis of the main results. Section 4 shows the simulation examples and Section 5 provides the conclusion.

Notations. $\mathbb{R}$ is the set of the real numbers. $\mathbb{R}^p$ and $\mathbb{R}^{p\times p}$ are the sets of the $p\times 1$ vectors and $p\times p$ real matrix, respectively. I_p is the p order identity matrix. $\mathrm{sign}(\cdot)$ is the sign function. $\|\cdot\|$ is the Euclidean norm.

2. Preliminaries and problem formulation

2.1. Graph theory

Let the interaction graph of the MANs be modeled as a directed graph $\mathcal{G}=\{\mathcal{V},\mathcal{E}\}$, where $\mathcal{V}=\{1,2,\ldots,N\}$ stands for the node set, $\mathcal{E}=\{(j,i)|i,j\in\mathcal{E}\}$ denotes the edge set. The adjacency matrix is defined as $\mathcal{A}=[a_{ij}]\in\mathbb{R}^{N\times N}$, where $a_{ij}>0$ if $(j,i)\in\mathcal{E}$ and $a_{ij}=0$ otherwise. In addition, self-loops are not allowed, i.e., $a_{ii}=0$. If the $\mathcal{G}$ is strongly connected, then there must be a directed path between each pair of nodes. A directed tree consists all nodes and edges. The $\mathcal{G}$ has a directed spanning tree, if there exists a leader node such that each of the followers has access to the signals of the leader by a directed path. The Laplacian matrix is defined as $\mathcal{L}=\mathcal{D}-\mathcal{A}$, where $\mathcal{D}=\mathrm{diag}(d_1,d_2,\ldots,d_N)$, $d_i=\sum_{j\in\mathcal{N}_i}a_{ij}$, and $\mathcal{N}_i$ is the neighbor set of the ith node. Besides, the matrix $\mathcal{B}=\mathrm{diag}(b_1,b_2,\ldots,b_N)$ is applied to represent the interaction between the leader and the ith follower. $b_i>0$ if there is an information flows directly from the leader to the ith follower and $b_i=0$ otherwise.

Assumption 1. The directed graph $\mathcal{G}$ has a spanning tree with the leader being the root, namely, there is at least one directed path from the leader to each follower.

Lemma 1 (*Zhang, Li, Qu, & Lewis, 2015*)**.** *Suppose that Assumption 1 holds. Then, there exists a positive define matrix* $\Xi=\mathrm{diag}(\xi_i)=\mathrm{diag}(y_i/x_i)$ *such that* $Q=\Xi H+H^T\Xi$ *is positive define, where* $y=[y_1,y_2,\ldots,y_N]^T=H^{-T}\mathbf{1}_N$, $x=[x_1,x_2,\ldots,x_N]^T=H^{-1}\mathbf{1}_N$, *and* $H=\mathcal{L}+\mathcal{B}$.

2.2. Lemmas

A time-varying function is proposed as follows (Song et al., 2017).

$$\eta(t)=\left(\frac{T_u}{t_0+T_u-t}\right)^{\rho},\ t\in[t_0,t_0+T_u)\,, \tag{1}$$

where ρ is a real number satisfying $\rho>1$, t_0 and T_u are the initial time and user-given settling time.

Consider the following system

$$\dot{y}(t)=f(t,y(t)),y_0=y(0), \tag{2}$$

where $y(t)\in\mathbb{R}^m$ is the state, $f:\mathbb{R}_+\times\mathbb{R}^m\to\mathbb{R}^m$ is a nonlinear vector bounded in time, y_0 is the initial state.

Definition 1 (*Ros & Teel, 2018*)**.** For system (2), the nonempty closed set $\mathcal{M}$ is finite-time attractive if there is a $T(y_0)>0$ such that $|y(t)|_{\mathcal{M}}=0$, $\forall t\geq T(y_0)$, where $T:\mathbb{R}^m\to[t_0,\infty)$ is the settling time function, $|y(t)|_{\mathcal{M}}$ represents the distance from $y(t)$ to $\mathcal{M}$, i.e., $|y(t)|_{\mathcal{M}}:=\inf_{r\in\mathcal{M}}|y(t)-r|$. Besides, $\mathcal{M}$ is fixed-time attractive for (2) if it is finite-time attractive and T is bounded by some constant $T_{\max}>0$.

Definition 2. The nonempty closed set $\mathcal{M}$ is prescribed-time attractive for system (2) if it is fixed-time attractive and there is a $T_u>0$ such that $|y(t)|_{\mathcal{M}}=0$, $\forall t\geq T_u$, where T_u is a time-independent constant and can be set arbitrarily. Besides, the function $T:\mathbb{R}^m\to[t_0,\infty)$ satisfies $\sup_{y_0\in\mathbb{R}^m}T(y_0)=t_0+T_u$, where t_0+T_u is the least upper bound of the function T.

Lemma 2 (*Ren et al., 2021*)**.** *There exists a Lyapunov function* $V(y)$ *for* (2) *such that*

$$\dot{V}(y)+cV(y)+k\psi(t)V(y)\leq 0,\ t\in[t_0,t_0+T_u), \tag{3}$$

where $c \geq 0$, $k > 0$, $\psi(t)$ is defined as

$$\psi(t) = \begin{cases} \frac{\dot{\eta}(t)}{\eta(t)}, & t_0 \leq t < t_0 + T_u, \\ \frac{\rho}{T_u}, & t \geq t_0 + T_u, \end{cases} \tag{4}$$

then the origin of system (2) is globally prescribed-time stable *with the prescribed-time $t_0 + T_u$. Especially, the following solution can be obtained.*

$$\begin{cases} V(y) \leq \eta(t)^{-k} \exp^{-c(t-t_0)} V(y_0), \ t \in [t_0, t_0 + T_u), \\ V(y) \equiv 0, t \in [t_0 + T_u, \infty). \end{cases} \tag{5}$$

Lemma 3 (*Wang, Yu, Yao, & Chen, 2018*)**.** *For a directed graph $\mathcal{G}$, it can be obtained that $y^T \Xi \mathcal{L} \text{sign}(y) \geq 0$, $\forall y = [y_1, y_2, \ldots, y_N]^T \in \mathbb{R}^N$.*

2.3. Control problem

Consider the second-order multi-agent network including N agents with the following dynamics.

$$\begin{aligned} \dot{x}_i(t) &= v_i(t), \\ \dot{v}_i(t) &= u_i(t), \ i \in \mathcal{V}, \end{aligned} \tag{6}$$

where $x_i(t), v_i(t) \in \mathbb{R}^r$ are the position and velocity states of the followers, r is the dimension of the states, and $u_i(t) \in \mathbb{R}^r$ is the control input.

Moreover, the dynamics of the leader is given as

$$\begin{aligned} \dot{x}_0(t) &= v_0(t), \\ \dot{v}_0(t) &= u_0(t), \end{aligned} \tag{7}$$

where $x_0(t), v_0(t) \in \mathbb{R}^r$ are the position and velocity of the leader, respectively, $u_0(t)$ is the control input or the acceleration of the leader.

Assumption 2. The states of the leader are bounded. There are some positive constants such that $\|x_0\| \leq \varpi_1$, $\|v_0\| \leq \varpi_2$, $\|u_0\| \leq \varpi_3$ and $\|\dot{u}_0\| \leq \varpi_4$.

Definition 3. The prescribed-time formation tracking problem of the second-order multi-agent network is solved if the tracking errors converge to zero within the prescribed-time T, namely,

$$\begin{cases} \lim_{t \to T} \|x_i(t) - x_0(t) - o_i\| = 0, \\ \|x_i(t) - x_0(t) - o_i\| = 0, \forall \ t > T, \\ \lim_{t \to T} \|v_i(t) - v_0(t)\| = 0, \\ \|v_i(t) - v_0(t)\| = 0, \forall \ t > T, \end{cases} \tag{8}$$

where $T > 0$ is an arbitrary time-independent constant, and o_i is the offset from the ith agent to the center of the formation shape.

3. Main results

In practical applications, it is unrealistic to assume that all the followers have access to the states of the leader. Assumption 1 implies that only a small part followers has directly access to the states of the leader, while the rest of the followers obtain leader's states by exchanging local interaction with their neighbors. A prescribed-time observer-based control algorithm is designed as

$$\begin{cases} \dot{\xi}_{ai} = -\beta \left(c + k\psi_1(t)\right) \zeta_{3i} - \gamma_1 \text{sign}(\zeta_{3i}), \\ \dot{\xi}_{vi} = \xi_{ai} - \beta \left(c + k\psi_2(t)\right) \zeta_{2i}, \\ \dot{\xi}_{xi} = \xi_{vi} - \beta \left(c + k\psi_3(t)\right) \zeta_{1i}, \end{cases} \tag{9a}$$

$$\begin{cases} \dot{x}_i = v_i, \\ \dot{v}_i = -k_1 \psi_4^2(t) \Big(\sum\limits_{j \in \mathcal{N}_i} a_{ij} (x_i - \xi_{xi} - o_i \\ \quad - (x_j - \xi_{xj} - o_j)) + b_i (x_i - \xi_{xi} - o_i) \Big) \\ \quad + \xi_{ai} - k_2 \psi_4(t) \Big(\sum\limits_{j \in \mathcal{N}_i} a_{ij} (v_i - \xi_{vi} \\ \quad - (v_j - \xi_{xj})) + b_i (v_i - \xi_{vi}) \Big), \end{cases} \tag{9b}$$

where $\zeta_{1i} = \sum_{j \in \mathcal{N}_i} a_{ij}(\xi_{xi} - \xi_{xj}) + b_i(\xi_{xi} - x_0)$, $\zeta_{2i} = \sum_{j \in \mathcal{N}_i} a_{ij}(\xi_{vi} - \xi_{vj}) + b_i(\xi_{vi} - v_0)$, $\zeta_{3i} = \sum_{j \in \mathcal{N}_i} a_{ij}(\xi_{ai} - \xi_{aj}) + b_i(\xi_{ai} - u_0)$, ξ_{xi}, ξ_{vi}, ξ_{ai} are the observed states of x_0, v_0, u_0, respectively. β, γ_1 are the observer gains, k_1, k_2 are the control parameters. $\psi_\iota(t)$ $(\forall \iota = 1, 2, 3, 4)$ is defined as

$$\psi_\iota(t) = \begin{cases} \frac{\dot{\eta}_\iota(t)}{\eta_\iota(t)}, & t_0 \leq t < t_0 + \iota T_u, \\ \frac{\rho}{\iota T_u}, & t \geq t_0 + \iota T_u, \end{cases}$$

where $\eta_\iota(t) = \left(\frac{\iota T_u}{t_0 + \iota T_u - t} \right)^\rho$, $t \in [t_0, t_0 + \iota T_u)$.

Remark 1. Different from the predefined-time state observers presented in Ni et al. (2021) and Ning and Han (2019), where the whole proof process is intricate and complex such that it is inconvenient to promote to solve related distributed problems. The proposed state observer has advantages including compact structure, simple theoretical derivation and the convergence time can be preset via tuning one parameter freely.

Theorem 1. *Suppose that Assumptions 1 and 2 hold. By using the prescribed-time observer-based control algorithm (9) for system (6), if*

$$\begin{aligned} &\gamma_1 > \varpi_4, \\ &\beta \geq \vartheta_2, \\ &\tfrac{2}{\rho} \leq k < \tfrac{k_1}{k_2}, \\ &k_1 \vartheta_2 - k_2^2 < 0, \\ &\vartheta_1 (4cT_u + k\rho + 1) + k_2 (2 + 4cT_u + k\rho) - \rho k_1 < 0, \\ &\vartheta_2 [k_1 (2\rho + 1) + (4cT_u + k\rho)(k_1 + k_2)] - \rho k_2^2 < 0, \end{aligned} \tag{10}$$

then the predefined-time formation tracking errors converge to zero within $T = t_0 + 4T_u$, where $\vartheta_1 = \frac{\lambda_{\max}(\Xi)}{\lambda_{\max}(Q)}$, $\vartheta_2 = \frac{\lambda_{\max}(\Xi)}{\lambda_{\min}(Q)}$.

Proof. The convergence analysis will be implemented by following two steps. First of all, let $\bar{\xi}_{ai} = \xi_{ai} - u_0$, $\bar{\xi}_a = \text{col}(\bar{\xi}_{a1}, \bar{\xi}_{a2}, \ldots, \bar{\xi}_{aN})$, $\zeta_3 = (H \otimes I_r)\bar{\xi}_a$. Then, it obtains the first equation (9a) as

$$\begin{aligned} \dot{\zeta}_3 = &-\beta(c + k\psi_1(t))(H \otimes I_r)\zeta_3 \\ &- \gamma_1 (H \otimes I_r) \text{sign}(\zeta_3) - (H \mathbf{1}_N \otimes \dot{u}_0). \end{aligned} \tag{11}$$

Consider the following Lyapunov function candidate $V_1 = \frac{1}{2} \zeta_3^T (\Xi \otimes I_r) \zeta_3$ and its derivative $\dot{V}_1 = -\beta(c + k\psi_1(t)) \zeta_3^T (\Xi H \otimes I_r)\zeta_3 - \gamma_1 \zeta_3^T (\Xi H \otimes I_r) \text{sign}(\zeta_3) - \zeta_3^T (\Xi H \mathbf{1}_N \otimes \dot{u}_0)$. Based on Lemma 3 and $\mathcal{L}\mathbf{1}_N = \mathbf{0}$, it can be obtained that

$$\begin{aligned} &- \zeta_3^T (\Xi H \otimes I_r) \text{sign}(\zeta_3) \\ &= -\zeta_3^T (\Xi \mathcal{L} \otimes I_r) \text{sign}(\zeta_3) - \zeta_3^T (\Xi \mathcal{B} \otimes I_r) \text{sign}(\zeta_3) \\ &\leq -\sum_{i=1}^N b_i \xi_i \|\zeta_{3i}\|, \end{aligned} \tag{12}$$

and

$$\begin{aligned} -\zeta_3^T (\Xi H \mathbf{1}_N \otimes \dot{u}_0) &= -\zeta_3^T (\Xi \mathcal{B} \mathbf{1}_N \otimes \dot{u}_0) \\ &\leq \sum_{i=1}^N b_i \xi_i \varpi_4 \|\zeta_{3i}\|. \end{aligned} \tag{13}$$

It thus follows that

$$\begin{aligned}\dot{V}_1 &\le -\tfrac{1}{2}\beta\lambda_{\min}(Q)(c+k\psi_1(t))\zeta_3^T\zeta_3 \\ &\quad -\sum_{i=1}^{N} b_i\xi_i(\gamma_1-\varpi_4)\|\zeta_{3i}\| \\ &\le -(c+k\psi_1(t))V_1,\end{aligned} \tag{14}$$

where $\gamma_1 > \varpi_4$ and $\beta \ge \vartheta_2$. From (4), $\psi_1(t) = \rho(t_0+T_u-t)^{-1}$, $t \in [t_0, t_0+T_u)$ and $\psi_1(t) = \rho T_u^{-1}$, $t \in [t_0+T_u, \infty)$, where $\rho > 1$, it can be obtained that $\psi_1(t)$ is always positive. Combining $c \ge 0$ with $k > 0$, it implies that $(c + k\psi_1(t))$ is always positive. It thus concludes that $\bar{\xi}_{ai}$ converges to the origin within $t_0 + T_u$ based on Lemma 2. When $t \ge t_0 + T_u$, $\bar{\xi}_{ai} \equiv 0$. Define $\bar{\xi}_{vi} = \xi_{vi} - v_0$, $\bar{\xi}_v = \mathrm{col}(\bar{\xi}_{v1}, \bar{\xi}_{v2}, \ldots, \bar{\xi}_{vN})$. Then, the second equation of (9a) can be rewritten as $\dot{\bar{\xi}}_v = -\beta(c + k\psi_2(t))(H \otimes I_r)\bar{\xi}_v$. Consider the following Lyapunov function candidate

$$V_2 = \frac{1}{2}\bar{\xi}_v^T(\Xi \otimes I_r)\bar{\xi}_v. \tag{15}$$

Taking the derivative of V_2 yields

$$\begin{aligned}\dot{V}_2 &= -\beta\,(c+k\psi_2(t))\,\bar{\xi}_v^T(\Xi H \otimes I_r)\bar{\xi}_v \\ &= -\tfrac{1}{2}\beta\,(c+k\psi_2(t))\,\bar{\xi}_v^T(Q \otimes I_r)\bar{\xi}_v \\ &\le -\tfrac{1}{2}\beta\,(c+k\psi_2(t))\,\lambda_{\min}(Q)\bar{\xi}_v^T\bar{\xi}_v.\end{aligned} \tag{16}$$

From (15), it can be obtained that $-1/2\lambda_{\max}(\Xi)\bar{\xi}_v^T\bar{\xi}_v \le -V_2 \le -1/2\lambda_{\min}(\Xi)\bar{\xi}_v^T\bar{\xi}_v$. It concludes that $-\bar{\xi}_v^T\bar{\xi}_v \le -2/\lambda_{\max}(\Xi)V_2$. Then, substituting these inequalities into (16), we obtain

$$\begin{aligned}\dot{V}_2 &\le -\beta\,(c+k\psi_2(t))\,\tfrac{\lambda_{\min}(Q)}{\lambda_{\max}(\Xi)}V_2 \\ &\le -(c+k\psi_2(t))V_2,\end{aligned}$$

where $-\beta\lambda_{\min}(Q)/\lambda_{\max}(\Xi) \le -1$, i.e., $\beta \ge \vartheta_2 = \lambda_{\max}(\Xi)/\lambda_{\min}(Q)$. It thus follows that $\bar{\xi}_{vi}$ converges to zero within $t_0 + 2T_u$. Similar to the steps (15) and (16), it can be obtained that $\bar{\xi}_{xi}$ converges to zero within $t_0 + 3T_u$. It can be derived that when $t \ge t_0 + 3T_u$, all the followers have access to the states of the leader.

Then, it is shown that for bounded initial values $x_i(t_0)$, $v_i(t_0)$, using (9b) for (6), the states $x_i(t)$, $v_i(t)$, $\forall i \in \mathcal{V}$ remain bounded when $t \in [t_0, t_0 + 3T_u)$. From (9a), it can be obtained that $\xi_{xi}(t)$, $\xi_{vi}(t)$, $\xi_{ai}(t)$ remain bounded for bounded initial values $\xi_{xi}(t_0)$, $\xi_{vi}(t_0)$, $\xi_{ai}(t_0)$, $\forall i \in \mathcal{V}$ when $t \in [t_0, t_0 + 3T_u)$. Besides, $\psi_1(t)$, $\psi_2(t)$, $\psi_3(t)$ are always bounded when $t \in [t_0, t_0 + 3T_u)$. Therefore, it can be concluded that $x_i(t)$, $v_i(t)$ remain bounded for bounded initial values $x_i(t_0)$, $v_i(t_0)$ when $t \in [t_0, t_0 + 3T_u)$.

Next, when $t \ge t_0 + 3T_u$, (9b) can be rewritten as

$$\begin{cases}\dot{x}_i = v_i, \\ \dot{v}_i = -k_1\psi_4^2(t)(\sum_{j\in\mathcal{N}_i} a_{ij}(x_i - x_0 - o_i \\ \quad -(x_j - x_0 - o_j)) + b_i(x_i - x_0 - o_i)) \\ \quad + u_0 - k_2\psi_4(t)(\sum_{j\in\mathcal{N}_i} a_{ij}(v_i - v_0 \\ \quad -(v_j - v_0)) + b_i(v_i - v_0)).\end{cases} \tag{17}$$

Let $\bar{x}_i = x_i - x_0 - o_i$, $\bar{v}_i = v_i - v_0$, $\bar{x} = \mathrm{col}(\bar{x}_1, \bar{x}_2, \ldots, \bar{x}_N)$, $\bar{v} = \mathrm{col}(\bar{v}_1, \bar{v}_2, \ldots, \bar{v}_N)$. Define two auxiliary states as

$$\tilde{x}_i = \psi_4(t)\bar{x}_i,\ \tilde{v}_i = \bar{v}_i. \tag{18}$$

By deriving $\tilde{x}_i$, it yields

$$\dot{\tilde{x}}_i = \tilde{\psi}_4(t)\tilde{x}_i + \psi_4(t)\tilde{v}_i, \tag{19}$$

where

$$\tilde{\psi}_4(t) = \frac{\dot{\psi}_4(t)}{\psi_4(t)} = \begin{cases}\frac{\psi_4(t)}{\rho}, & t_0 \le t < t_0 + 4T_u, \\ 0, & t \ge t_0 + 4T_u.\end{cases} \tag{20}$$

Then, it can be obtained that

$$\begin{cases}\dot{\tilde{x}} = \tilde{\psi}_4(t)\tilde{x} + \psi_4(t)\tilde{v}, \\ \dot{\tilde{v}} = -\psi_4(t)(H \otimes I_r)(k_1\tilde{x} + k_2\tilde{v}),\end{cases} \tag{21}$$

where $\tilde{x} = \mathrm{col}[\tilde{x}_1, \tilde{x}_2, \ldots, \tilde{x}_N)$, $\tilde{v} = \mathrm{col}(\tilde{v}_1, \tilde{v}_2, \ldots, \tilde{v}_N)$. Define $Y = [\tilde{x}^T, \tilde{v}^T]^T$. It follows that

$$\dot{Y} = \Omega Y, \tag{22}$$

where

$$\Omega = \begin{bmatrix}\tilde{\psi}_4(t)I_N & \psi_4(t)I_N \\ -k_1\psi_4(t)H & -k_2\psi_4(t)H\end{bmatrix} \otimes I_r.$$

The Lyapunov function candidate is constructed as

$$V_3 = \frac{1}{2}Y^T(\Phi \otimes I_r)Y, \tag{23}$$

where

$$\Phi = \begin{bmatrix}k_1 Q & \frac{k_1}{k_2}\Xi \\ \frac{k_1}{k_2}\Xi & \Xi\end{bmatrix},$$

Q, Ξ are defined in Lemma 1. From Lemma 1, it obtains that Ξ is positive define, then according to the fourth inequality of (10), it follows that $V_3 \ge 0$.

Taking the derivative of V_3 along (21), it follows that

$$\begin{aligned}\dot{V}_3 &= \tfrac{k_1}{\rho}\psi_4(t)\tilde{x}^T(Q \otimes I_r)\tilde{x} - \tfrac{k_1^2}{k_2}\psi_4(t)\tilde{x}^T(H\Xi \otimes I_r)\tilde{x} \\ &\quad + \tfrac{k_1}{k_2}\psi_4(t)\tilde{v}^T(\Xi \otimes I_r)\tilde{v} - k_2\psi_4(t)\tilde{v}^T(H\Xi \otimes I_r)\tilde{v} \\ &\quad + \tilde{x}^T\left(k_1\psi_4(t)(Q \otimes I_r) + \tfrac{k_1}{k_2\rho}\psi_4(t)(\Xi \otimes I_r)\right)\tilde{v} \\ &\quad - k_1\psi_4(t)\tilde{x}^T(Q \otimes I_r)\tilde{v}.\end{aligned} \tag{24}$$

By means of Lemma 1, the following equality holds.

$$\begin{aligned}\tfrac{k_1^2}{k_2}\psi_4(t)\tilde{x}^T(H\Xi \otimes I_r)\tilde{x} &= \tfrac{k_1^2}{2k_2}\psi_4(t)\tilde{x}^T(Q \otimes I_r)\tilde{x}, \\ k_2\psi_4(t)\tilde{v}^T(H\Xi \otimes I_r)\tilde{v} &= \tfrac{k_2}{2}\psi_4(t)\tilde{v}^T(Q \otimes I_r)\tilde{v}.\end{aligned} \tag{25}$$

It thus follows

$$\begin{aligned}\dot{V}_3 &= \psi_4(t)\left(\tfrac{k_1}{\rho} - \tfrac{k_1^2}{2k_2}\right)\tilde{x}^T(Q \otimes I_r)\tilde{x} \\ &\quad + \psi_4(t)\left(\tfrac{k_1}{k_2}\tilde{v}^T(\Xi \otimes I_r)\tilde{v} - \tfrac{k_2}{2}\tilde{v}^T(Q \otimes I_r)\tilde{v}\right) \\ &\quad + \tfrac{k_1}{k_2\rho}\psi_4(t)\tilde{x}^T(\Xi \otimes I_r)\tilde{v}.\end{aligned} \tag{26}$$

Based on Lemma 1 and Young's inequality, it can be easily concluded that

$$\begin{aligned}&\lambda_{\min}(Q)\tilde{x}^T\tilde{x} \le \tilde{x}^T(Q \otimes I_r)\tilde{x} \le \lambda_{\max}(Q)\tilde{x}^T\tilde{x}, \\ &\tilde{x}^T(\Xi \otimes I_r)\tilde{v} \le \tfrac{1}{2}\lambda_{\max}(\Xi)\left(\tilde{x}^T\tilde{x} + \tilde{v}^T\tilde{v}\right).\end{aligned} \tag{27}$$

Substituting (27) into (26) yields

$$\begin{aligned}\dot{V}_3 &\le \left[\left(\tfrac{k_1}{\rho} - \tfrac{k_1^2}{2k_2}\right)\lambda_{\max}(Q) + \tfrac{k_1}{k_2\rho}\lambda_{\max}(\Xi)\right] \\ &\quad \times \psi_4(t)\tilde{x}^T\tilde{x} - \tfrac{k_2}{2}\lambda_{\min}(Q)\psi_4(t)\tilde{v}^T\tilde{v} \\ &\quad + \tfrac{k_1}{k_2}\lambda_{\max}(\Xi)\left(1 + \tfrac{1}{2\rho}\right)\psi_4(t)\tilde{v}^T\tilde{v}.\end{aligned} \tag{28}$$

According to (23) and (27), it can be obtained that

$$\begin{aligned}V_3 &\le \tfrac{k_1}{2}\lambda_{\max}(Q)\tilde{x}^T\tilde{x} + \tfrac{1}{2}\lambda_{\max}(\Xi)\tilde{v}^T\tilde{v} \\ &\quad + \tfrac{k_1}{2k_2}\lambda_{\max}(\Xi)\left(\tilde{x}^T\tilde{x} + \tilde{v}^T\tilde{v}\right) \\ &= \left(\tfrac{k_1}{2}\lambda_{\max}(Q) + \tfrac{k_1}{2k_2}\lambda_{\max}(\Xi)\right)\tilde{x}^T\tilde{x} \\ &\quad + \left(\tfrac{k_1}{2k_2} + \tfrac{1}{2}\right)\lambda_{\max}(\Xi)\tilde{v}^T\tilde{v}.\end{aligned} \tag{29}$$

Define $R_1(t) = \dot{V}_3 + (c + k\psi_4(t))V_3$. From (4), it implies that $0 < 1/\psi_4(t) \le 4T_u/\rho$. Let $R_1(t) \le 0$. It follows that

$$\begin{aligned} R_1(t) \le & \frac{k_1}{2k_2\rho}[(k_2(2+4cT_u+k\rho)-\rho k_1)\lambda_{\max}(Q) \\ & + (4cT_u+k\rho+1)\lambda_{\max}(\Xi)]\tilde{x}^T\tilde{x} \\ & + \frac{1}{2k_2\rho}[-\rho k_2^2\lambda_{\min}(Q)+k_1(2\rho+1)\lambda_{\max}(\Xi) \\ & + (4cT_u+k\rho)(k_1+k_2)\lambda_{\max}(\Xi)]\tilde{v}^T\tilde{v} \\ & \le 0. \end{aligned} \tag{30}$$

It can be obtained that the conditions (10) hold. It thus concludes that $\dot{V}_3 \le -cV_3 - k\psi_4(t)V_3$. According to Lemma 2, it follows

$$V_3 \le \eta_4^{-k}(t)\exp^{-c(t-t_0)}V_3(t_0). \tag{31}$$

Note the fact that

$$\begin{aligned} \left\|\tilde{x}\right\|^2 + \|\tilde{v}\|^2 &= \psi_4^2(t)\|\bar{x}\|^2 + \|\bar{v}\|^2 \\ &\ge \delta_1\left(\|\bar{x}\|^2 + \|\bar{v}\|^2\right), \end{aligned} \tag{32}$$

where $\delta_1 = \min\left\{\rho^2/16T_u^2, 1\right\}$.

Based on (29) and (31), one has

$$\left\|\tilde{x}\right\|^2 + \|\tilde{v}\|^2 \le \frac{1}{\delta_2}\eta_4^{-k}(t)\exp^{-c(t-t_0)}V_3(t_0), \tag{33}$$

where $\delta_2 = \lambda_{\max}(\Xi)\min\{\frac{k_1}{2\vartheta_1} + \frac{k_1}{2k_2}, \frac{k_1}{2k_2} + \frac{1}{2}\}$.

Combining (32) with (33), it obtains

$$\|\bar{x}\|^2 + \|\bar{v}\|^2 \le \frac{1}{\delta_1\delta_2}\eta_4^{-k}(t)\exp^{-c(t-t_0)}V_3(t_0). \tag{34}$$

Based on Lemma 2, it obtains $\lim_{t\to T}\eta_4^{-k}(t) = 0$, where $T = t_0 + 4T_u$. It further obtains $\lim_{t\to T}\|\bar{x}\| = 0$ and $\lim_{t\to T}\|\bar{v}\| = 0$. For $t \in [T, \infty)$, it can be obtained that $V_3 \equiv 0$. It thus concludes that $\|\bar{x}\| = \|\bar{v}\| \equiv 0$. Namely, the prescribed-time formation tracking is achieved within $T = t_0 + 4T_u$.

For $t \in [t_0, T)$, according to (17) and (21), it obtains the control input $u = u_0 \otimes \mathbf{1}_r - \psi_4(t)(H \otimes I_r)(k_1\tilde{x} + k_2\tilde{v})$, where $u = \mathrm{col}(u_1, u_2, \ldots, u_N)$. According to Young's inequality and (34), it can be obtained that

$$\begin{aligned} & \|k_1\tilde{x} + k_2\tilde{v}\| \\ & \le [(k_1^2 + k_1k_2)\|\tilde{x}\|^2 + (k_2^2 + k_1k_2)\|\tilde{v}\|^2]^{\frac{1}{2}} \\ & \le \epsilon_1(\|\tilde{x}\|^2 + \|\tilde{v}\|^2)^{\frac{1}{2}} \\ & \le \frac{\epsilon_1}{\delta_1\delta_2}\eta_4^{-\frac{k}{2}}(t)\exp^{-\frac{c}{2}(t-t_0)}V_3^{\frac{1}{2}}(t_0), \end{aligned}$$

where $\epsilon_1 = \max\{\sqrt{k_1^2 + k_1k_2}, \sqrt{k_2^2 + k_1k_2}\}$. Note that

$$\begin{aligned} \psi_4(t)\eta_4^{-\frac{k}{2}}(t) &= \frac{\rho}{t_0+4T_u-t}\frac{(t_0+4T_u-t)^{0.5k\rho}}{(4T_u)^{0.5k\rho}} \\ &= \frac{\rho}{4T_u}\left(\frac{t_0+4T_u-t}{4T_u}\right)^{0.5(k\rho-2)}. \end{aligned}$$

If $k\rho - 2 \ge 0$, it means that $\psi_4(t)\eta_4^{-\frac{k}{2}}(t) \le \frac{\rho}{4T_u}$. Besides, $0 < \exp^{-\frac{c}{2}(t-t_0)} \le 1$. It follows that

$$\|u\| \le \varpi_3 + \frac{\rho\epsilon_1}{4\delta_1\delta_2T_u}V_3^{\frac{1}{2}}(t_0).$$

It thus concludes that the control input u is bounded for bounded initial value $V_3(t_0)$. For $t \ge T$, $\tilde{x} = \tilde{v} \equiv 0$, $\|u\| \le \varpi_3$. It thus concludes that the control input u_i is bounded over $t \in [t_0, \infty)$. This completes the proof.

Remark 2. In Ning et al. (2019), the TBG-based approach is proposed to address the leader-following consensus under the assumption that the interaction graph is detailed-balanced. The proposed control algorithm solves the formation tracking problem under the assumption that the directed interaction graph contains a spanning tree. From the aspect of graph theory, the latter assumption is less conservative comparing with the former. Besides, we also present Corollary 2 to show the corresponding result in the case of detailed-balanced graphs. Moreover, different from the fact that the convergence time of the TBG-based approach depends on a time-varying function with multiple constraints, the presented algorithm allows the users to arbitrarily determine the convergence time by selecting a specific parameter. However, the presented algorithm in this paper is still constrained by the fact that faster convergence generally leads to higher control cost.

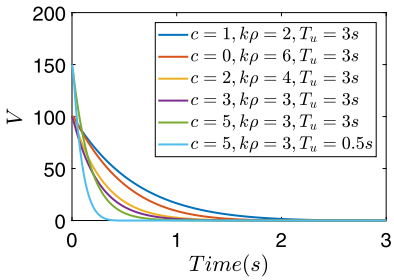

Fig. 1. The evolution of V with the parameters c, k, ρ, T_u.

Remark 3. The conditions (10) can be rewritten as

$$\begin{aligned} \frac{\lambda_{\max}(\Xi)}{\lambda_{\min}(Q)} &< \sigma k_2, \\ \frac{\lambda_{\max}(\Xi)}{\lambda_{\max}(Q)} &< \frac{(1-\sigma k)\rho-2-cT_1}{cT_1+k\rho+1}\frac{k_2}{\sigma}, \\ \frac{\lambda_{\max}(\Xi)}{\lambda_{\min}(Q)} &< \frac{\rho k_2\sigma}{2\rho+1+(cT_1+k\rho)(1+\sigma)}, \end{aligned} \tag{35}$$

where $\sigma = k_2/k_1$, $1 - \sigma k > 0$ and $T_1 = 4T_u$. Note that the parameters c, k, T_u, ρ are the self-selected constants. Under Assumption 1, it can be obtained $\lambda_{\max}(\Xi), \lambda_{\max}(Q), \lambda_{\min}(Q)$ are some positive constants. By using the trail-and-error method, we can find a large enough k_2 with a positive constant σ such that the conditions (35) hold without needing the matrices Q and Ξ.

Remark 4. In order to choose the appropriate control gains of Theorem 1, the process of tuning parameters is shown as follows. (1) Set the interaction graph $\mathcal{G}$ and initialize parameters ρ, t_0, T_u, c and k. (2) Calculate the parameters $\lambda_{\max}(\Xi), \lambda_{\max}(Q)$ and $\lambda_{\min}(Q)$ based on the given directed graph $\mathcal{G}$. (3) Define $\sigma = \frac{k_2}{k_1}$, initialize σ and search an appropriate k_2 such that the sign of the fourth, fifth and sixth inequality of (10) is equal to -1. It thus obtains the value of k_2 and k_1.

Remark 5. Fig. 1 shows the evolution of V with c, k, ρ, T_u, where $t_0 = 0.01$ s, $c \ge 0$, $k > 0$ and $k\rho \ge 2$, the condition k, ρ is obtained based on (10). The following conclusions could be drawn. (1) A greater increase $c + k\rho$ suggests more rapid convergence speed. (2) When $c + k\rho$ is a fixed value, the larger c is, the more rapid convergence speed is. (3) The convergence time of V is independent of the parameters c, k, ρ and initial condition, which can be set freely by selecting the parameter T_u.

Remark 6. Consider that each follower suffers from the unknown and bounded disturbances $d_i(t)$. The related dynamics is described as

$$\begin{aligned} \dot{x}_i(t) &= v_i(t), \\ \dot{v}_i(t) &= u_i(t) + d_i(t). \end{aligned}$$

In order to eliminate the effect of the disturbances, a fixed-time observer is proposed as

$$\begin{cases} \dot{z}_{i1} = z_{i2} - n_1 \mathrm{sig}^{a_1}(z_{i1} - x_i) - m_1 \mathrm{sig}^{b_1}(z_{i1} - x_i), \\ \dot{z}_{i2} = z_{i3} - n_2 \mathrm{sig}^{a_2}(z_{i1} - x_i) - m_2 \mathrm{sig}^{b_2}(z_{i1} - x_i) + u_i, \\ \dot{z}_{i3} = -n_3 \mathrm{sig}^{a_3}(z_{i1} - x_i) - m_3 \mathrm{sig}^{b_3}(z_{i1} - x_i), \end{cases}$$

where z_{i1}, z_{i2}, z_{i3} are the observer states of x_i, v_i, d_i, respectively. $1 - \varepsilon_1 < a_1 < 1$, $a_2 = 2a_1 - 1$, $a_3 = 3a_1 - 2$, $1 < b_1 < 1 + \varepsilon_2$, $b_2 = 2b_1 - 1$, $b_3 = 3b_1 - 2$, $0 < \varepsilon_1, \varepsilon_2 \ll 1$ are two small numbers. $n_1, n_2, n_3, m_1, m_2, m_3$ are the observer parameters, $\mathrm{sig}^p(x) = |x|^p \,\mathrm{sign}(x)$. Define the observer errors as $\varrho_{i1} = z_{i1} - x_i$, $\varrho_{i2} = z_{i2} - v_i$, $\varrho_{i3} = z_{i3} - d_i$. It then obtains the following error dynamics

$$\begin{cases} \dot{\varrho}_{i1} = \varrho_{i2} - n_1 \mathrm{sig}^{a_1}(\varrho_{i1}) - m_1 \mathrm{sig}^{b_1}(\varrho_{i1}), \\ \dot{\varrho}_{i2} = \varrho_{i3} - n_2 \mathrm{sig}^{a_2}(\varrho_{i1}) - m_2 \mathrm{sig}^{b_2}(\varrho_{i1}), \\ \dot{\varrho}_{i3} = -n_3 \mathrm{sig}^{a_3}(\zeta_{i1}) - m_3 \mathrm{sig}^{b_3}(\varrho_{i1}). \end{cases}$$

Based on Theorem 2 of Basin, Yu, and Shtessel (2017), the observer errors $\varrho_{i1}, \varrho_{i2}, \varrho_{i3}$ converge to zero in fixed time. However, how to force the disturbance estimation errors to converge to the origin in prescribed time deserves further investigation in the future.

Remark 7. It is worth mentioning that the proposed prescribed-time control protocol has divided the main control process into several end-to-end sub-processes. The settling time of each sub-process can be prescribed arbitrarily in theory and is thus regardless of the initial time and condition. Thus, the convergence and ending of one sub-process implies the activation and beginning of the next. It thus motivates the theoretical analysis of the prescribed-time convergence for the main process.

Remark 8. The design idea of the control protocol (9a) and (9b) mainly lies on the sufficient using of the real-time states and the estimated states of the neighboring agents. The advantage of such manner can improve the dynamic performance of the real-time states for each agent especially in the case that the estimated states contain high overshoot or transient errors due to the sufficient employment of the real-time states. In this sense, we newly present such a control protocol and leave the possibility of applying it in the case that the dynamics of the estimator and the agents are highly distinguished.

In the following corollary, some extended prescribed-time control problems are presented based on the solution to Theorem 1, including the prescribed-time formation tracking with the undirected graphs and detailed-balanced directed graphs.

Corollary 1. *Suppose that the interaction graph $\mathcal{G}$ is undirected and Assumptions 1 and 2 hold. The prescribed-time formation tracking problem can be solved within the prescribed-time $T = t_0 + 4T_u$ by utilizing the algorithm (9) for system (6), if the following conditions hold.*

$$\begin{aligned} &\gamma_1 > \varpi_4, \\ &\beta \geq \vartheta_2, \\ &k\rho \geq 2, \\ &4T_u(1 + c) + \rho(k - k_1) \leq 0, \\ &4T_u(\lambda_{\max}(H) + c) + \rho[k - k_1\lambda_{\max}(H) \\ &\quad - 2k_2\lambda_{\min}(H)] \leq 0. \end{aligned} \tag{36}$$

Proof. Consider the following Lyapunov function $V_4 = \frac{1}{2}\tilde{x}^T(H \otimes I_r)\tilde{x} + \frac{1}{2}\tilde{v}^T\tilde{v}$. The derivative of V_4 along (21) yields $\dot{V}_4 = (1 - k_1\psi_4(t))\tilde{x}^T(H \otimes I_r)\tilde{v} - k_2\psi_4(t)\tilde{v}^T(H \otimes I_r)\tilde{v}$. Note that $\tilde{x}^T(H \otimes I_r)\tilde{v} \leq \frac{\lambda_{\max}(H)}{2}\left(\tilde{x}^T\tilde{x} + \tilde{v}^T\tilde{v}\right)$ and $V_4 \leq \frac{1}{2}\lambda_{\max}(H)\tilde{x}^T\tilde{x} + \frac{1}{2}\tilde{v}^T\tilde{v}$. Let $R_2(t) = \dot{V}_4 + (c + k\psi_4(t))V_4$. It follows that

$$\begin{aligned} R_2(t) \leq\ & \tfrac{1}{2}\lambda_{\max}(H)[1 + c + (k - k_1)\psi_4(t)]\tilde{x}^T\tilde{x} \\ & + \tfrac{1}{2}[(k - k_1\lambda_{\max}(H) - 2k_2\lambda_{\min}(H)) \\ & \times \psi_4(t) + \lambda_{\max}(H) + c]\tilde{v}^T\tilde{v}. \end{aligned} \tag{37}$$

If the conditions (36) hold, it implies that $R_2(t) \leq 0$. It thus obtains that $\dot{V}_4 \leq -(c + k\psi_4(t))V_4$. Similar to the analysis steps of (28)–(34), it follows that $\lim_{t\to T}\|\tilde{x}\| = 0$, $\lim_{t\to T}\|\tilde{v}\| = 0$ and $\|\tilde{x}\| = \|\tilde{v}\| = 0, \forall\, t \geq T$. The reset analysis is similar to that of Theorem 1 and omitted here.

Corollary 2. *Suppose that the interaction graph $\mathcal{G}$ is detailed-balanced and Assumption 1 holds. The prescribed-time formation tracking problem can be solved within the prescribed-time $T = t_0 + 4T_u$ by utilizing the algorithm (9) for system (6), if the following conditions hold.*

$$\begin{aligned} &\gamma_1 > \varpi_4, \\ &\beta \geq \vartheta_2, \\ &k\rho \geq 2, \\ &4T_u(1 + c) + \rho(k - k_1) \leq 0, \\ &4T_u[\lambda_{\max}(\Gamma) + c\lambda_{\max}(\Upsilon)] + \rho[k\lambda_{\max}(\Upsilon) \\ &\quad - k_1\lambda_{\max}(\Gamma) - 2k_2\lambda_{\min}(\Gamma)] \leq 0. \end{aligned} \tag{38}$$

Proof. Based on Theorem 1 Lu, Lu, Chen, and Lu (2013), if the $\mathcal{G}$ is detailed-balanced and has a spanning tree with the leader as the root, there exist some positive constants γ_i such that $\gamma_i a_{ij} = \gamma_j a_{ji}$ for all $i, j \in \mathcal{V}$. Besides, it obtains that $\Gamma = \Upsilon H$ is symmetric and positive definite, where $\Upsilon = \mathrm{diag}(\gamma_1, \gamma_2, \ldots, \gamma_N)$. Consider the following Lyapunov function $V_5 = \frac{1}{2}\tilde{x}^T(\Gamma \otimes I_r)\tilde{x} + \frac{1}{2}\tilde{v}^T(\Upsilon \otimes I_r)\tilde{v}$. The derivative of V_5 is $\dot{V}_5 = (1 - k_1\psi_4(t))\tilde{x}^T(\Gamma \otimes I_r)\tilde{v} - k_2\psi_4(t)\tilde{v}^T(\Gamma \otimes I_r)\tilde{v}$. Let $R_3(t) = \dot{V}_5 + (c + k\psi_4(t))V_5$. It can be obtained that

$$\begin{aligned} R_3(t) \leq\ & \tfrac{1}{2}\lambda_{\max}(\Gamma)[1 + c + (k - k_1)\psi(t)]\tilde{x}^T\tilde{x} \\ & + \tfrac{1}{2}[(k\lambda_{\max}(\Upsilon) - k_1\lambda_{\max}(\Gamma) \\ & - 2k_2\lambda_{\min}(\Gamma))\psi(t) + \lambda_{\max}(\Gamma) \\ & + c\lambda_{\max}(\Upsilon)]\tilde{v}^T\tilde{v}. \end{aligned} \tag{39}$$

If the conditions (38) hold, it implies that $R_3(t) \leq 0$. It obtains that $\dot{V}_5 \leq -(c + k\psi_4(t))V_5$. Similar to the analysis steps of (28)–(34), it follows that $\lim_{t\to T}\|\tilde{x}\| = 0$, $\lim_{t\to T}\|\tilde{v}\| = 0$ and $\|\tilde{x}\| = \|\tilde{v}\| = 0, \forall\, t \geq T$. The reset analysis is similar to that of Theorem 1 and omitted here.

4. Illustrative examples

In this section, several simulation examples are carried out to investigate the effectiveness of the proposed algorithms. Consider that the multi-agent networks are composed of six agents with the interaction graph in Fig. 2, whose adjacency weights are set to 1, $\forall (j, i) \in \mathcal{E}$. Let $\mathcal{B} = \mathrm{diag}(1, 0, 0, 0, 0, 1)$. Then, the corresponding eigenvalues are obtained as $\lambda_{\max}(Q) = 10.6155$, $\lambda_{\min}(Q) = 0.4679$ and $\lambda_{\max}(\Xi) = 5$. Let $\rho = 6$, $t_0 = 0.01$ s, $T_u = 0.75$ s, $k = 0.5$, $c = 1$. It can be concluded that $\vartheta_1 = 0.4710$, $\vartheta_2 = 10.6861$. Based on Remark 4, let $\sigma = 0.5$. According to (10), let

$$\begin{aligned} c_1 &= \vartheta_2 - \sigma k_2, \\ c_2 &= \sigma\vartheta_1(4cT_u + k\rho + 1) + k_2[\sigma(2 + 4cT_u + k\rho) - \rho], \\ c_3 &= \vartheta_2[2\rho + 1 + (4cT_u + k\rho)(1 + \sigma)] - \rho\sigma k_2. \end{aligned}$$

Then, search an appropriate k_2 from $[0, 50]$ such that the parameters c_1, c_2, c_3 are negative. The evolution of the parameters c_1, c_2, c_3 is shown in Fig. 3. It can be obtained that when $k_2 >$

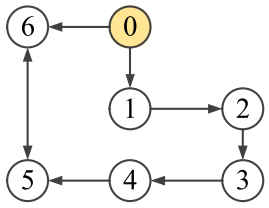

Fig. 2. The interaction graph of multi-agent systems.

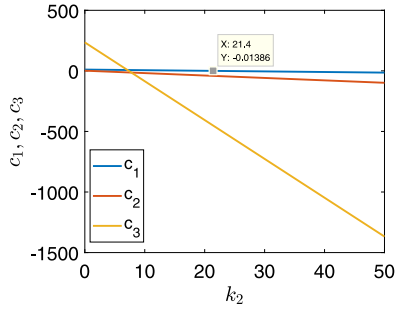

Fig. 3. The evolution of parameters c_1, c_2, c_3.

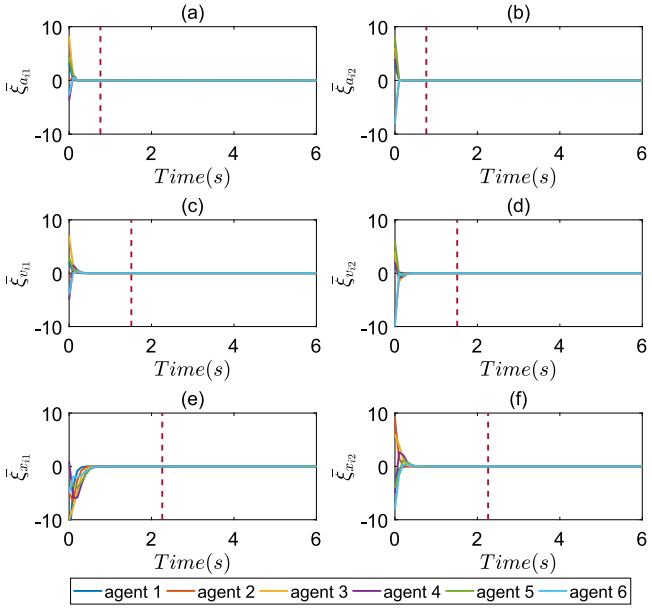

Fig. 4. Pictures (a) (b), pictures (c) (d) and pictures (e) (f) show the observer errors $\bar{\xi}_{ai}$, $\bar{\xi}_{vi}$ and $\bar{\xi}_{xi}$ converge to zero within the prescribed-time t_0+T_u, t_0+2T_u and t_0+3T_u, respectively.

21.4, all the parameters c_1, c_2, c_3 are negative. It thus selects $k_1 = 60, k_2 = 30$.

The role of the virtual leader is to provide the trajectory for all the followers. The trajectory of the virtual leader is described as

$$\begin{cases} x_0 = [2 + 5\cos(0.5t), -1 + 4\sin(0.5t)]^T, \\ v_0 = [-2.5\sin(0.5t), 2\cos(0.5t)]^T, \\ u_0 = [-1.25\cos(0.5t), -\sin(0.5t)]^T. \end{cases}$$

The formation offsets are given as

$$\begin{cases} R = 1, o_1 = R[1, 0]^T, o_2 = R[\cos(\frac{\pi}{3}), \sin(\frac{\pi}{3})]^T, \\ o_3 = R[-\cos(\frac{\pi}{3}), \sin(\frac{\pi}{3})]^T, o_4 = R[-1, 0]^T, \\ o_5 = -R[\cos(\frac{\pi}{3}), \sin(\frac{\pi}{3})]^T, o_6 = R[\cos(\frac{\pi}{3}), -\sin(\frac{\pi}{3})]^T. \end{cases}$$

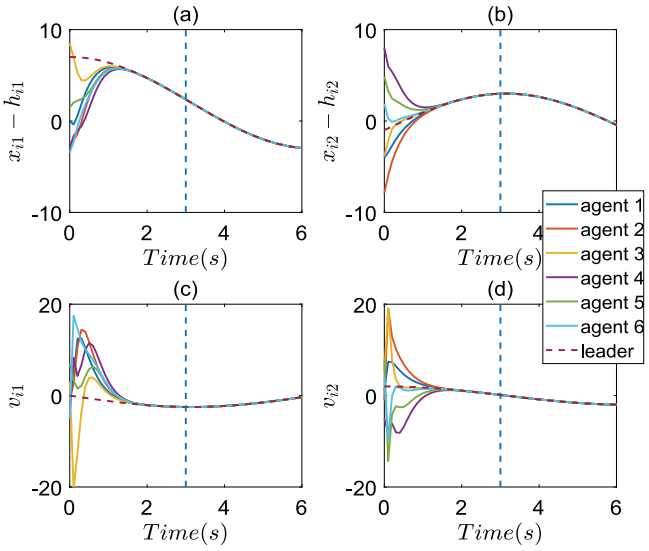

Fig. 5. Pictures (a) (b) and pictures (c) (d) show the evolution of the states of x_i and v_i, respectively.

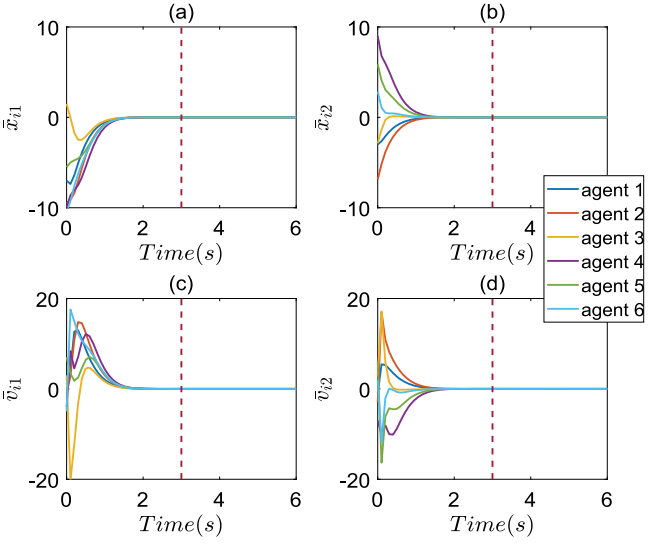

Fig. 6. Pictures (a) (b) and pictures (c) (d) show the formation tracking errors $\bar{x}_i$ and $\bar{v}_i$ converge to zero within the prescribed-time T, respectively.

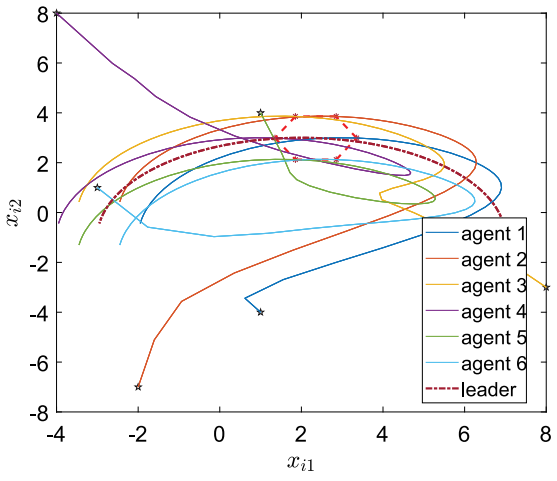

Fig. 7. Formation shape formed by all the agents at $t = 3.01$ s, where $\star$ represent the initial positions of all agents, $*$ is the position states of all the agents at $t = 3.01$ s.

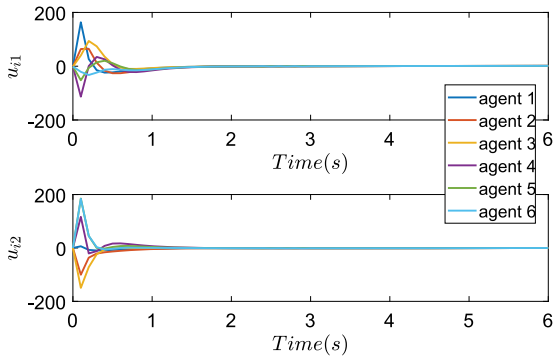

Fig. 8. The evolution of the control input u_i.

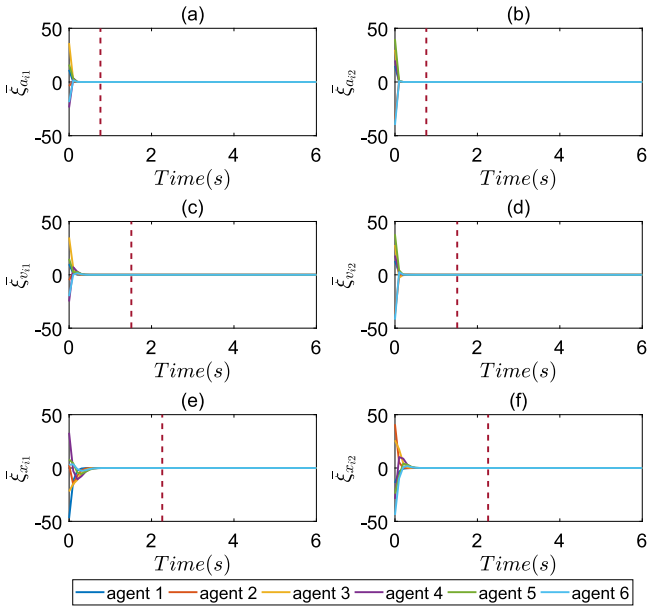

Fig. 9. Pictures (a) (b), pictures (c) (d) and pictures (e) (f) show the observer errors $\bar{\xi}_{ai}$, $\bar{\xi}_{vi}$ and $\bar{\xi}_{xi}$ converge to zero within the prescribed-time t_0+T_u, t_0+2T_u and t_0+3T_u, respectively.

Besides, it can be obtained from (10) that $\gamma_1 = 1, \beta = 11$. The ideal convergence time is $T = t_0 + 4T_u = 3.01$ s.

Example 1. The initial values of x_i, v_i, ξ_{xi}, ξ_{vi}, ξ_{ai} are selected randomly from $[-10,10]$. Applying the algorithm (9) for (6), the simulation results are shown in Figs. 4–8. Fig. 4 shows that the observer errors $\bar{\xi}_{ai}$, $\bar{\xi}_{vi}$ and $\bar{\xi}_{xi}$ converge to zero within the prescribed-time t_0+T_u, t_0+2T_u and t_0+3T_u, respectively. Figs. 5–6 show that the states x_i, v_i approach the trajectory of the leader within T. Fig. 7 depicts the formation tracking control objective has been achieved within T. Fig. 8 indicates that the control input remains bounded at $t \in [t_0, \infty)$.

Example 2. The initial values of x_i, v_i, ξ_{xi}, ξ_{vi}, ξ_{ai} are selected five times larger than ones defined in Example 1. Then, the simulation results are shown in Figs. 9–12. Fig. 9 shows that the observer errors $\bar{\xi}_{ai}$, $\bar{\xi}_{vi}$ and $\bar{\xi}_{xi}$ converge to zero within the prescribed-time $t_0 + T_u$, $t_0 + 2T_u$ and $t_0 + 3T_u$, respectively. 10 shows that the formation tracking errors converge to the origin within T. Figs. 4, 6, 8, 10 indicate that the convergence-time of the proposed prescribed-time observer-based control algorithm is independent of the initial states. Fig. 11 depicts the formation tracking performance. Fig. 12 shows the control input is bounded

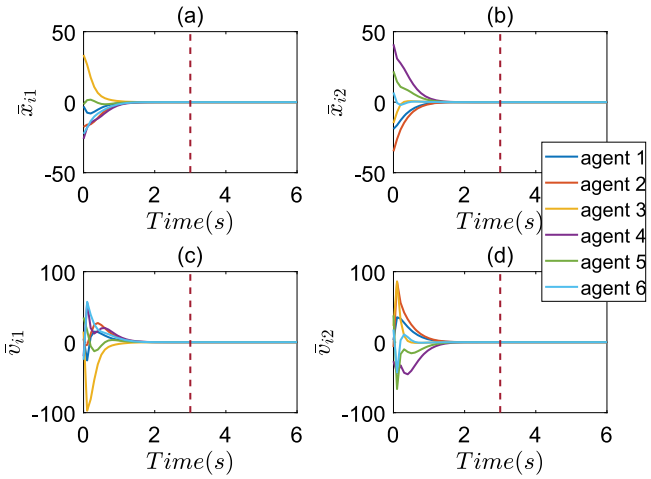

Fig. 10. Pictures (a) (b) and pictures (c) (d) show the formation tracking errors $\bar{x}_i$ and $\bar{v}_i$ converge to zero within the prescribed-time T, respectively.

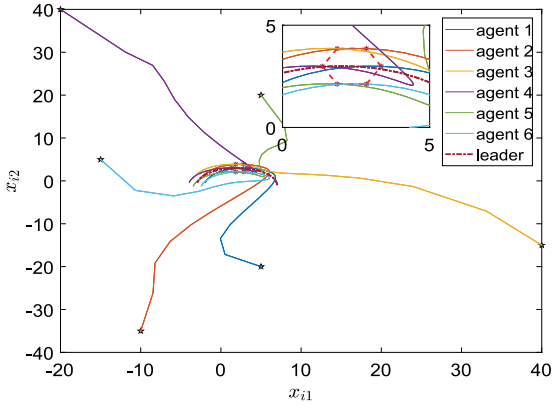

Fig. 11. Formation shape formed by all the agents at $t = 3.01$ s, where $\star$ represent the initial positions of all agents, $*$ is the position states of all the agents at $t = 3.01$ s.

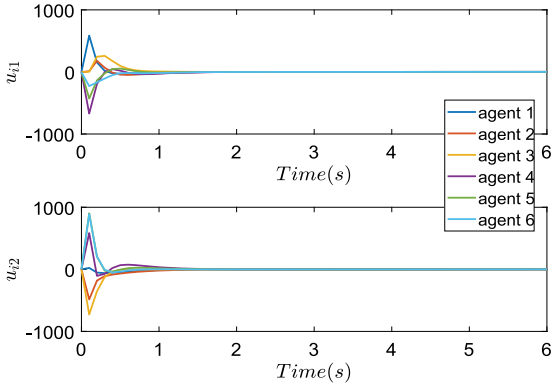

Fig. 12. The evolution of the control input u_i.

over $t \in [t_0, \infty)$. All the above-mentioned results demonstrate the effectiveness of the proposed control algorithm (9).

5. Conclusion

This paper has studied the prescribed-time formation tracking problem of second-order multi-agent networks with directed graphs. A new state observer has been designed such that the

observer errors converge to the origin in prescribed-time, which can be preset in advance via tuning a time-independent parameter freely. Then, several prescribed-time observer-based control algorithms have been developed to successfully solve the formation tracking problem. A novel constructed Lyapunov function is presented to demonstrate the stability of the closed-loop system, such that the structure of sufficient condition is more simpler and easier to obtain the control parameters. The effectiveness of the presented algorithms have been demonstrated by several illustrative examples.

Acknowledgments

This work was supported in part by the National Natural Science Foundation of China under Grants 62073301, 52027806, 62233007, and 61973133, in part by the National Key Technology R&D Program of China under Grant 2020YFB1709301 and Grant 2020YFB1709304, in part by the Natural Science Foundation of Hubei Province of China under Grants 2021CFB516 and 2022CFA052, in part by the Innovative Development Project for Supporting Enterprise Technology of Hubei Province of China under Grant 2021BAB094.

References

Basin, M., Yu, P., & Shtessel, Y. (2017). Finite- and fixed-time differentiators utilising HOSM techniques. *IET Control Theory & Applications*, *11*(8), 1144–1152.

Cai, Y., Zhang, H., Wang, Y., Zhang, J., & He, Q. (2021). Fixed-time time-varying formation tracking for nonlinear multi-agent systems under event-triggered mechanism. *Information Sciences*, *564*, 45–70.

Chen, X., Yu, H., & Hao, F. (2020). Prescribed-time event-triggered bipartite consensus of multiagent systems. *IEEE Transactions on Cybernetics*, http://dx.doi.org/10.1109/TCYB.2020.3004572.

Ding, T. F., Ge, M. F., Liu, Z. W., Wang, Y. W., & Karimi, H. R. (2020). Lag-bipartite formation tracking of networked robotic systems over directed matrix-weighted signed graphs. *IEEE Transactions on Cybernetics*, http://dx.doi.org/10.1109/TCYB.2020.3034108.

Du, H., Wen, G., Wu, D., Cheng, Y., & Lu, J. (2020). Distributed fixed-time consensus for nonlinear heterogeneous multi-agent systems. *Automatica*, *113*, Article 108797.

Ge, M. F., Guan, Z. H., Yang, C., Li, T., & Wang, Y. W. (2016). Time-varying formation tracking of multiple manipulators via distributed finite-time control. *Neurocomputing*, *202*(19), 20–26.

Ge, M. F., Liu, Z. W., Wen, G., Yu, X., & Huang, T. (2020). Hierarchical controller-estimator for coordination of networked Euler–Lagrange systems. *IEEE Transactions on Cybernetics*, *50*(6), 2450–2461.

Holloway, J., & Krstic, M. (2019a). Prescribed-time observers for linear systems in observer canonical form. *IEEE Transactions on Automatic Control*, *64*(9), 3905–3912.

Holloway, J., & Krstic, M. (2019b). Prescribed-time output feedback for linear systems in controllable canonical form. *Automatica*, *107*, 77–85.

Hong, H., Yu, W., Wen, G., & Yu, X. (2017). Distributed robust fixed-time consensus for nonlinear and disturbed multiagent systems. *IEEE Transactions on Systems, Man, and Cybernetics: Systems*, *47*(99), 1464–1473.

Hua, Y., Dong, X., Liang, H., Li, Q., & Ren, Z. (2020). Finite-time time-varying formation tracking for high-order multiagent systems with mismatched disturbances. *IEEE Transactions on Systems, Man, and Cybernetics: Systems*, *50*(10), 3795–3803.

Khoo, S., Xie, L., & Man, Z. (2009). Robust finite-time consensus tracking algorithm for multirobot systems. *IEEE/ASME Transactions on Mechatronics*, *14*(2), 219–228.

L, S., Du, H., & Lin, X. (2011). Finite-time consensus algorithm for multi-agent systems with double-integrator dynamics. *Automatica*, *47*(8), 1706–1712.

Liang, C. D., Ge, M. F., Liu, Z. W., Ling, G., & Liu, F. (2020). Predefined-time formation tracking control of networked marine surface vehicles. *Control Engineering Practice*, *107*, Article 104682.

Liang, X., Liu, Y. H., Wang, H., Chen, W., Xing, K., & Liu, T. (2016). Leader-following formation tracking control of mobile robots without direct position measurements. *IEEE Transactions on Automatic Control*, *61*(12), 4131–4137.

Lu, X., Lu, R., Chen, S., & Lu, J. (2013). Finite-time distributed tracking control for multi-agent systems with a virtual leader. *IEEE Transactions on Circuits and Systems. I. Regular Papers*, *60*(2), 352–362.

Lv, Y., Wen, G., & Huang, T. (2020). Adaptive protocol design for distributed tracking with relative output information: a distributed fixed-time observer approach. *IEEE Transactions on Control of Network Systems*, *7*(1), 118–128.

Ni, J., Liu, L., Tang, Y., & Liu, C. (2021). Predefined-time consensus tracking of second-order multiagent systems. *IEEE Transactions on Systems, Man, and Cybernetics: Systems*, *51*(4), 2550–2560.

Ning, B., & Han, Q. L. (2019). Prescribed finite-time consensus tracking for multi-agent systems with nonholonomic chained-form dynamics. *IEEE Transactions on Automatic Control*, *64*(4), 1686–1693.

Ning, B., Han, Q. L., & Zuo, Z. (2019). Practical fixed-time consensus for integrator-type multi-agent systems: a time base generator approach. *Automatica*, *105*, 406–414.

Ning, B., Han, Q. L., & Zuo, Z. (2021). Bipartite consensus tracking for second-order multi-agent systems: a time-varying function based preset-time approach. *IEEE Transactions on Automatic Control*, *66*(6), 2739–2745.

Olfati-Saber, R., & Murray, R. M. (2004). Consensus problems in networks of agents with switching topology and time-delays. *IEEE Transactions on Automatic Control*, *49*(9), 1520–1533.

Polyakov, A. (2012). Nonlinear feedback design for fixed-time stabilization of linear control systems. *IEEE Transactions on Automatic Control*, *57*(8), 2106–2110.

Ren, W., & Beard, R. W. (2005). Consensus seeking in multiagent systems under dynamically changing interaction topologies. *IEEE Transactions on Automatic Control*, *50*(5), 655–661.

Ren, Y., Zhou, W., Li, Z., Liu, L., & Sun, Y. (2021). Prescribed-time cluster lag consensus control for second-order non-linear leader-following multiagent systems. *ISA Transactions*, *109*, 49–60.

Ros, H., & Teel, A. R. (2018). A hybrid fixed-time observer for state estimation of linear systems. *Automatica*, *87*, 103–112.

Song, Y., Wang, Y., Holloway, J., & Krstic, M. (2017). Time-varying feedback for regulation of normal-form nonlinear systems in prescribed finite time. *Automatica*, *83*, 243–251.

Tian, B., Lu, H., Zuo, Z., & Yang, W. (2019). Fixed-time leader-follower output feedback consensus for second-order multiagent systems. *IEEE Transactions on Cybernetics*, *49*(4), 1545–1550.

Wang, Y., Song, Y., Hill, D. J., & Krstic, M. (2019). Prescribed-time consensus and containment control of networked multiagent systems. *IEEE Transactions on Cybernetics*, *49*(4), 1138–1147.

Wang, H., Yu, W., Yao, L., & Chen, G. (2018). Fully-distributed finite-time consensus of second-order multi-agent systems on a directed network. In *2018 IEEE international symposium on circuits and systems*. http://dx.doi.org/10.1109/ISCAS.2018.8351776.

Wang, Y., Yuan, Y., & Liu, B. (2021). Finite-time leader-following output consensus for multi-agent systems via extended state observer. *Automatica*, *124*, Article 109133.

Wen, G., Yu, X., Fu, J., Wang, H., & Yu, W. (2021). Fast distributed average tracking in multi-agent networks: the case with general linear agent dynamics. *IEEE Transactions on Control of Network Systems*, *8*(2), 997–1009.

Xiao, F., Wang, L., Chen, J., & Gao, Y. (2009). Finite-time formation control for multi-agent systems. *Automatica*, *45*(11), 2605–2611.

Yang, H., & Ye, D. (2020). Distributed fixed-time consensus tracking control of uncertain nonlinear multiagent systems: a prioritized strategy. *IEEE Transactions on Cybernetics*, *50*(6), 2627–2638.

Yoo, S. J., & Kim, T. H. (2015). Distributed formation tracking of networked mobile robots under unknown slippage effects. *Automatica*, *54*, 100–106.

You, X., Hua, C. C., Li, K., & Jia, X. (2020). Fixed-time leader-following consensus for high-order time-varying nonlinear multiagent systems. *IEEE Transactions on Automatic Control*, *65*(12), 5510–5516.

Zhang, H., Li, Z., Qu, Z., & Lewis, F. L. (2015). On constructing Lyapunov functions for multi-agent systems. *Automatica*, *58*, 39–42.

Zhao, L. W., & Hua, C. C. (2014). Finite-time consensus tracking of second-order multi-agent systems via nonsingular TSM. *Nonlinear Dynamics*, *75*(1–2), 311–318.

Zuo, Z. (2014). Non-singular fixed-time terminal sliding mode control of non-linear systems. *IET Control Theory & Applications*, *9*(4), 545–552.

Zuo, Z. (2015). Nonsingular fixed-time consensus tracking for second-order multi-agent networks. *Automatica*, *54*, 305–309.

Teng-Fei Ding received the B.S. degree in mechanical design, manufacturing and automation in 2011, the M.S.degree mechanical engineering in 2014, and the Ph.D. degree in Geological Equipment Engineering in 2022 from China University of Geosciences, Wuhan, China.

He is currently a lecturer with the School of Mechanical Engineering and Electronic Information, China University of Geosciences, Wuhan. His current research interests include networked robotic systems, distributed control and optimization.

Ming-Feng Ge received his B.S. degree in automatic control in 2004 and the Ph.D. degree in control theory and control engineering in 2016 both from Huazhong University of Science and Technology, China.

He is currently a Professor with the School of Mechanical Engineering and Electronic Information, China University of Geosciences, Wuhan. He is also a Visiting Scholar with the School of Automation, Central South University, Changsha. His research interests include networked robotic systems, distributed control and human-in-the-loop systems.

Caihua Xiong received the Ph.D. degree in mechanical engineering from the Huazhong University of Science and Technology (HUST), Wuhan, China, in 1998. From 1999 to 2003, he was with the City University of Hong Kong, Hong Kong, and the Chinese University of Hong Kong, Hong Kong, as a Postdoctoral Fellow, and Worcester Polytechnic Institute, Worcester, MA, USA, as a Research Scientist. He is currently a Chang Jiang Professor and Director of the Institute of Rehabilitation and Medical Robotics at HUST. His research interests include biomechatronic prostheses, rehabilitation robotics, and robot motion planning and control.

Zhi-Wei Liu received the B.S. degree in information management and information system from Southwest Jiaotong University, Chengdu, China, in 2004 and the Ph.D. degree in control science and engineering from the Huazhong University of Science and Technology, Wuhan, China, in 2011.

He is currently a Professor with the School of Artificial Intelligence and Automation, Huazhong University of Science and Technology. His current research interests include cooperative control and optimization of distributed network systems.

Guang Ling received the M.S. degree in Probability Theory and Mathematical Statistics from Huazhong University of Science and Technology in 2007, and the Ph.D. degree in control theory and control engineering from Huazhong University of Science and Technology, Wuhan, China, in 2016.

He is currently an Associate Professor in the School of Science, Wuhan, China. His research interests include complex systems and complex networks, data mining and machine learning.